Application of Three Dimensional Laser-Two-Focus Anemometry to Unsteady Flow in a Transonic Turbine Stage

Freudenreich K.
Tel: + 46 8 790 7480
kai@egi.kth.se

Fransson T. H.
Tel: + 46 8 790 7475
fransson@egi.kth.se

Fax: + 46 8 204161
The Royal Institute of Technology
Chair of Heat and Power Technology
10044 Stockholm
Sweden

ABSTRACT

A project has been started to investigate the effect of stator induced flow distortions on the aeromechanical excitation of downstream rotor blades in transonic turbine flow. Detailed experiments are supposed to be a basis for the evaluation of numerical codes that are planned to serve as design tools. The wind tunnel for rotating cascades (RGG), a high pressure cold flow test turbine at the German Aerospace Center (DLR) in Göttingen, has been used as the test facility.
The objective of the presented experiments is the investigation of the unsteady velocity flow field between stator and rotor and throughout the rotor passage. A state-of-the-art three dimensional Laser-Two-Focus Anemometer (3D-L2F) has been employed to measure the 3D mean velocity vector and the turbulence intensity field at midspan.
The application of the 3D-L2F to unsteady turbomachinery measurements is explained. Occurring problems are described, as with the seeding, the optical access and the clear identification of geometrical positions. Examples of the required data acquisition time are given. An analysis of the factors influencing the measurement accuracy is carried out and a few results are presented.

NOMENCLATURE

c	[-]	Weighting factor in eq. (2)
e	[m/s], [°]	Accuracy range
N	[-]	Number of TOF events
R	[mm]	Radial coordinate
Tu	[-]	Turbulence intensity
$\lvert\vec{V}_{2D}\rvert$	[m/s]	2D velocity vector magnitude
x	[mm]	Axial coordinate
α	[°]	Flow angle
γ	[°]	Inclination angle to optical axis
σ	[m/s], [°]	Standard deviation
σ_B^2/A	[-]	Noise level ratio
Φ	[rad]	Circumferential coordinate
χ	[°]	Radial flow angle

Abbreviations

DEHS	Diethylhexylsebacat
DLR	German Aerospace Center
KTH	The Royal Institute of Technology
L2F	Laser-Two-Focus Anemometer
LDA	Laser-Doppler-Anemometer
RGG	Wind Tunnel for Rotating Cascades
RPM	Revolutions Per Minute
SNR	Signal-to-Noise-Ratio
TOF	Time-Of-Flight

INTRODUCTION

Upstream stator induced vortical and potential fields can result in serious vibration problems for turbine rotors, if these disturbances are experienced with the blade eigenfrequencies. For the unsteady blade forces and moments the unsteady blade surface pressures are of importance. For the coupling between stator induced flow defects and the resulting unsteady rotor surface pressures the unsteady flow field from the stator throughout the rotor passage is of significant importance as well. Investigations of the unsteady velocity flow field of turbomachines have proven Laser-Doppler-Anemometry (LDA) and especially Laser-Two-Focus Anemometry (L2F) to be very valuable techniques to obtain detailed and accurate flow information, without disturbing the flow by a physical probe head. So far, Walraevens and Gallus [1995] and Zaccaria and Lakshminarayana [1997] used LDA, while Binder et al. [1985] and Kost et al. [2000] used L2F, all for two dimensional investigations in subsonic turbine stages. Applications of 3D-L2F systems to compressor tests were reported by eg. Maass et al. [1994], Beversdorff et al. [1998] and Vouillarmet and Charpenel [1998].

OBJECTIVES

The aim of this presentation is to explain the use of a 3D-L2F system for transonic turbine stage experiments, including occurring problems, the data acquisition times, the accuracy range analysis and a few results.

TEST FACILITY AND TEST OBJECTS

The experiments were performed in the wind tunnel for rotating cascades (RGG), a high pressure cold flow test turbine at the German Aerospace Center (DLR) in Göttingen. The RGG is a continuous mode closed loop facility. A 1 MW variable speed electric motor drives a 4 stage radial compressor, providing a constant flow rate of 15.5 m^3/s and a maximum pressure ratio of 6. Both Mach and Reynolds number can be varied independently within a certain range. A combination of a vacuum pump and a high pressure air feed is used to adjust the static pressure level, while the temperature is controlled by a water-cooled heat exchanger. A rotor can be either driven in both direction with up to 10.000 RPM or braked using a 500 kW motor/generator. The entire test facility is controlled and monitored by an industrial "Simatic S5" control system. It is able to keep the rotor turning frequency within an accuracy range of ± 1 RPM, about ± 0.015% for the present case. A schematic sketch of the facility is given in Fig. 1. Further details can be found in Amecke and Kost [1993].

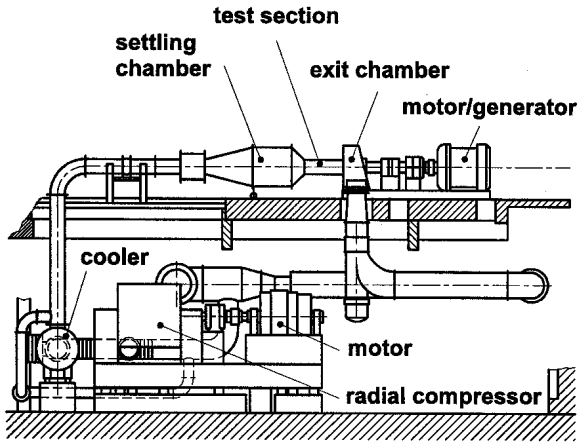

Fig. 1: *The wind tunnel for rotating cascades RGG*

A quartz glass window is inserted in the test section casing to provide optical access for laser anemometry over the tip of the airfoils. For stator wake traverses the circumferential measurement location of a laser anemometer or a probe is kept constant, while the stator can be rotated over approximately two pitches. Stator and rotor rotate in an abrasive material embedded in the casing. This provides a tight connection between airfoil tips and casing. A once-per-revolution signal from the rotor axis can be used to trigger the acquisition of unsteady data, as for laser anemometry, hot film or unsteady pressure transducers.
For the presented investigations the test section was equipped with an aero-engine size transonic high pressure turbine stage. A 43 vane stator was run with a 64 blade rotor. The stator vanes are cylindrical, while the rotor blades have 3D shape. Figure 2 shows the stage and the measurement positions at 50% span, the rotor tip section is superposed. Data were taken at high subsonic and transonic stator exit flow conditions.

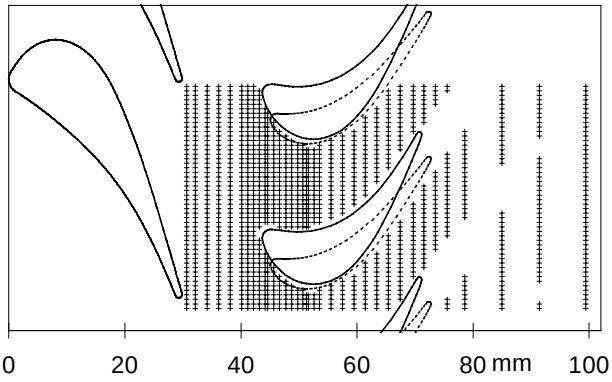

Fig. 2: *Stage geometry at 50% span (—), rotor at tip (---)and measurement positions (+++)*

3D LASER-TWO-FOCUS ANEMOMETER

During the last almost 25 years the L2F has become a well established technique in the turbomachinery domain. Due to its non-intrusive nature it is especially suited for high velocity measurements in narrow flow channels. A two dimensional L2F is able to detect the velocity components in the plane perpendicular to the laser beams. It works as a light gate. Small oil droplets traveling with the flow pass two focused laser beams with known distance. The particles scatter light, which is observed by photo detectors. With the measured time delay between the two impulses, the time-of-flight (TOF) and the foci distance the particle velocity is calculated. The second focus point is rotated stepwise around the first one to detect the main flow angle α. At each step a few hundred to several thousand TOF events are detected for a sufficient statistical analysis. The obtained flow quantities are the 2D velocity vector magnitude $\left|\vec{V}_{2D}\right|$, the flow angle α and the turbulence intensity Tu. Comprehensive reviews about the technique and its applications were given by Schodl [1980 and 1986]. Successful applications for turbomachinery investigations were reported by Binder et al. [1985], Kost [1992a], Trebinjac et al. [1993], Gieß and Kost [1997] and Kost et al. [2000].

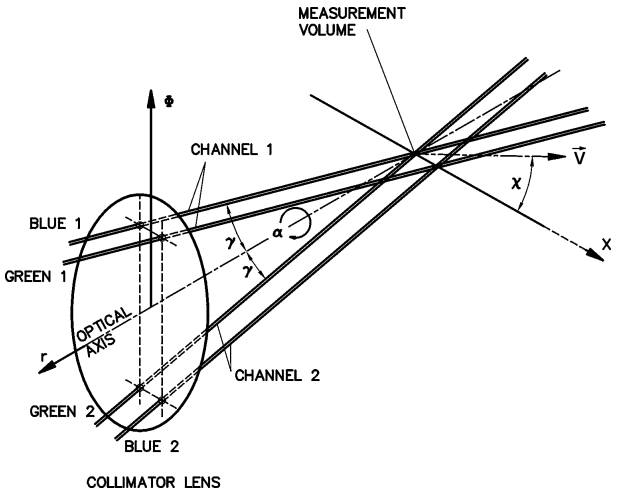

Fig. 3: *3D-L2F optical configuration*

The first working 3D-L2F system was presented by Förster et al. [1990]. Here, the same measurement volume is observed by two single L2F systems, channel 1 and 2, from different angles of incidence. The two channels are inclined by about $\gamma = \pm 7.5°$ from the main optical axis, see Fig. 3. If the flow includes a radial component, along the main optical axis, both systems detect different flow angles $\alpha_{channel\ 1}$ and $\alpha_{channel\ 2}$. From this difference the radial flow angle χ is calculated. The calculation is very sensitive to the exact geometric adjustment of channel 1 and 2 to each other. Required geometrical parameters are obtained from a calibration, see Maass et al. [1994]. The mean 2D velocity vector magnitude $\left|\vec{V}_{2D}\right|$, the flow angle α and the turbulence intensity Tu are calculated to be the arithmetic mean of the two single systems. The 3D velocity vector magnitude results from

$$\left|\vec{V}_{3D}\right| = \left|\vec{V}_{2D}\right| / \cos(\chi) \qquad (1)$$

As a previous step of the presented experiments the 3D-L2F was applied to stator only measurements in the RGG [Freudenreich and Fransson 1998, Freudenreich et al. 1999]. Examples of successful rotating turbomachinery applications of 3D-L2F systems were given by Maass et al. [1994], Beversdorff et al. [1998] and Vouillarmet and Charpenel [1998].

UNSTEADY DATA ACQUISITION

Rotor only Configuration

For measurements in a rotor only configuration and at a fixed axial and radial position only one geometrical parameter must be considered. This is the instantaneous circumferential position of the measurement volume relative to the rotor. During the experiments the volume was kept at constant circumferential position, coordinate Φ, while the rotor was rotating. The unsteady data sampling was triggered by a one-per-revolution impulse from the rotor axis. To keep the data acquisition time within reasonable limits, data from all 64 rotor passages were superposed to obtain one representative passage. The one-per-revolution signal was multiplied to obtain a one-per-blade signal. Whenever a TOF event was successfully evaluated, the phase lag to the last one-per-blade trigger signal was recorded. To refer the TOF event to a position within the rotor passage the rotor pitch was subdivided into 32 equally spaced increments ("windows"). This describes the spatial resolution in the rotor relative coordinate system, see Fig. 4. The event was then assigned to that window, which covered the phase lag TOF event-trigger signal. To be more specific, this data acquisition should be called "periodic", instead of "unsteady". For a detailed description see Schodl [1980].
The position of the 32 windows inside the blade pitch needs to be known. A useful geometric paramter is the phase lag from the trigger to the leading edge. Kost [1996] described the procedure to determine this. Velocity measurements are simulated with the solid blade as the "particles". The measurement volume is positioned at the blade tip of the rotating rotor. When the blades pass the volume, strong reflections are caused at the suction and pressure side edges of the blade. These reflections are assigned to the respective windows. This procedure was performed at 28 positions along the rotor axial chord. An envelope resulted, describing the blade tip contour. The actual blade tip contour was placed onto this envelope using a least square fit. The phase lag trigger-leading edge could be calculated. Figure 4 shows one blade pitch covered by the 32 windows,

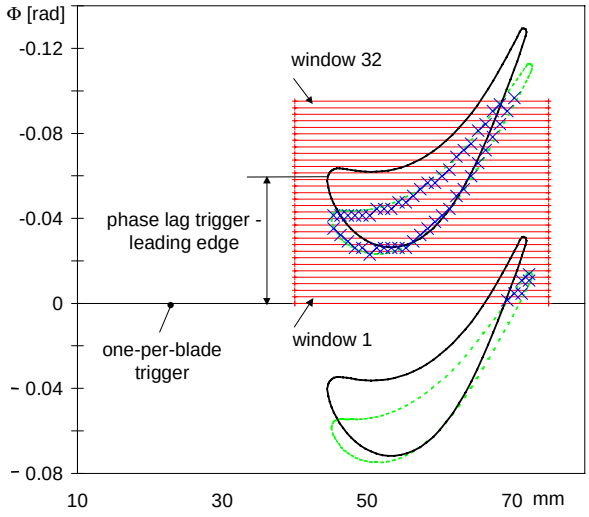

Fig. 4: *Determination of the phase lag one-per-blade trigger signal to leading edge, rotor at 50% span (—), rotor at tip (---)*

the envelope describing the blade tip and the actual blade contours at tip and at midspan. The circumferential resolution of the envelope is 1/32 of the rotor pitch per single axial position. But the repetition of the procedure at 28 positions resulted in an accuracy range better than ± 0.05 % blade pitch for the phase lag trigger-leading edge.
It is of high importance that this procedure is carried out for the final rotor speed and axial loading. In the RGG the encoder for the one-per-revolution signal from the rotor axis is located about 2 m away from the rotor, towards the motor/generator. Differences in speed and axial loading induced a changing twist of the rotor axis over this 2 m distance. The maximum twist/untwist that occurred between two different operating points was 0.0113 rad or 11.5% of a rotor pitch.

Stator-Rotor Configuration

If the rotor inlet conditions are steady and uniform in circumferential direction, Φ, the flow in the rotor relative frame of reference is steady. An upstream stator introduces non-homogeneous flow in (at least) the circumferential direction. Seen from the moving rotor relative frame of reference the stator vanes are passing by, causing unsteady flow conditions in the rotor relative frame of reference. To capture this unsteady (periodic) flow condition, a second geometrical parameter must be considered. This is the circumferential position of the measurement volume relative to the upstream stator, the stator indexing. To cover the complete stator influence onto the rotor, the above described procedure (for the rotor only case) must be repeated for several positions of the measurement volume relative to the stator, covering at least one stator pitch. The number of stator index positions describes the temporal resolution of the flow in the rotor relative frame of reference. The number of windows per rotor pitch describes the spatial resolution within the rotor passage. For a detailed description of this procedure see Förster et al. [1986].
As mentioned above, to change the circumferential position of the measurement volume relative to the stator the measurement volume was kept at a fixed position, while the stator was indexed. For the presented experiments slightly more than one stator pitch was covered by indexing the stator at 22 positions relative to the measurement volume. This resulted in 0.007 rad steps. The indexing mechanism had an accuracy of ± 0.00035 rad (= 0.25% stator pitch) what was considered to be sufficient. The 22 stator steps were interpolated to about 48 steps to match the step width to the width of a single rotor window. The final measurement grid can be seen as a combination of Fig. 2 and Fig. 4. In Fig. 2 the grid is seen from the absolute stator frame of reference, in Fig. 4 from the rotor relative frame of reference. As for the rotor, it was assumed that all stator passages were identical. Only one stator passage was investigated in detail. Minor influence from obviously differently shaped trailing edges could be noticed.
This procedure results in a fairly long data acquisition time. To inspect the flow at a fixed axial and radial position data were taken at 22 stator indexing positions. For each position all 32 windows per rotor pitch were filled up with a sufficient number of TOF events. This required about 1-2 h for positions in the axial gap and in the front rotor passage. About 4-5 h was required for positions in the rear rotor passage and especially downstream of the rotor. The differences were mostly due to different seeding and optical access conditions.
The described unsteady data acquisition procedure worked fairly straightforward. Significant problems did not occur.

SEEDING

The RGG is a closed loop facility run with dried air. To obtain a sufficient particle rate in the measurement volume the airstream was seeded artificially. Schodl [1980] studied the ability of particles of different density and diameter to follow the flow over shock waves. He concluded that for oil substances a diameter smaller than 0.3 μm is required to follow the flow almost instantaneously. For the presented experiments Diethylhexylsebacat (DEHS), a synthetic non-toxic and non-flammable oil, was used. An aerosol generator produced particles with a mean diameter of 0.08-0.1 μm, the percentage of particles larger than 0.3 μm was neglectible. For a high data rate the guidance of the particles to the measurement volume was of specific importance. The particles were injected into the settling chamber. A 6 mm diameter L-type tube, turned in downstream direction, was connected to a probe traverse mechanism. By careful control of the probe traverse mainly those streamlines were seeded that passed the measurement volume.
However, some difficulties occurred. Low seeding rates were obtained in near wake regions. Wake fluid originates mainly from the airfoil boundary layers, into which seeding particles rarely migrate. Near wake regions showed also high levels of turbulence intensity due to alternate separation of the trailing edge vortices and mixing processes with the main flow. The 3D-L2F needs to cover a large angular sector to detect the main flow angle α. Both low seeding and high Tu caused low data rates and long measurement times. Successful measurements were performed as close as 0.8 mm downstream of the stator trailing edge. No attempt was made to get closer. Further downstream, in the axial gap and in the front rotor passage the seeding conditions improved, since

the low particle stator wakes mixed out. In the rear rotor passage and especially downstream of the rotor the seeding density in the measurement volume decreased. This resulted from unsteady flow structures distorting the seeded streamlines. A large region at the rear rotor suction side could not be investigated, see Fig. 2. Missing optical acces as a reason could be excluded, see next chapter. This low seeded area might be caused by the passage vortices sweeping the rear suction side. They consist mainly of low seeded boundary layer fluid. Downstream of the rotor superposition of stator and rotor wake and vortex fluid occurred, enforcing the problem of low seeding. Measurements in the near rotor wake region were impossible. The first axial position downstream of the rotor, where enough seeding was found along the entire stator and rotor passage, was about one axial rotor chord.
A second problem occurred during rotor downstream measurements. Seeding particles impinged onto the rotor blades. They accumulated and were driven towards the tip trailing edge. Large oil droplets were spilled off the rotor trailing edge and impinged onto the window, creating an oil coating. This caused disturbing laser light reflections. During rotor downstream measure-ments the window needed to be dismounted and cleaned about every second to third day.
The data acquisition time depended strongly on the seeding conditions, including the oil coating on the window. The shortest acquisition time was experienced in the axial gap and front rotor passage. In the near stator wake the time doubled approximately, in the rotor downstream region it was approximately three to four times as long.

OPTICAL ACCESS

Optical access was given through a quartz glass window (quality: BK7) inserted in the casing over the airfoils tips. This plane-parallel 8 mm thick window had an axial extension of 100 mm and a circumferential extension of 15 mm. For safety reasons a small gap of about 0.4 mm was kept between the stator and rotor design tip and the window. A small step of about 0.7 mm existed between the plane parallel window and the curved casing. The blade span is about 35 mm. During previous experiments in the RGG no detectable influence of this step on the flow was found at positions ≥10% flow channel height behind the window [Gieß and Kost 1997].
In Fig. 2 and 4 it can be seen that the rotor tip section covers parts of the rotor front and rear suction side passage at midspan, where the flow was investigated. At these positions the laser beams would be blocked by the rotor tips if the main optical axis of the 3D-L2F would be radially orientated. Similar problems occur at the stator trailing edge. To avoid this, at these axial locations the optical axis was inclined by 15° to the radial direction. At the rotor leading edge the laser beams pointed slightly downstream and slightly upstream at the stator and rotor trailing edges. Especially at the rotor leading edge measurements could be performed extremely close to the surface, see Fig. 2. At the rotor trailing edge the improved optical access did not provide better results. Measurements were obviously prohibited by a lack of seeding.
Seriously disturbing reflections from stray light at the solid blade surfaces were not experienced. The laser beams were “blanked” when the blades passed the measurement volume. This was done by shutting off the beams in those windows which were covered by the blades, see Fig. 4.

ADJUSTMENT OF THE 3D-L2F TO THE RGG

Figure 5 shows the 3D-L2F positioned in front of the test section. The optical head is mounted on a 3D traversing system that is supported by a heavy frame. The optical head is connected to the laser, the photo detectors and the signal processing unit via fiber and electrical connections, as well as the traverse. The entire system is automatically controlled by a PC. The optical head/traverse/frame and the RGG rest on different

Fig. 5: *3D-L2F in front of test section and iced diffusion chamber on right hand side*

foundations, thus they are mechanically decoupled. Any vibrations from the wind tunnel would not affect the measurement system. On the right hand side of Fig. 5, downstream of the test section, a completely iced diffusion chamber can be seen. The blue paint appears only at the de-iced print. This was caused by the extraction of enthalpy by the flow driven rotor. A decrease of 65-70 K in the absolute total temperature over the rotor resulted in an absolute total temperature downstream of the rotor of 240-245 K. During operation the moisture of the lab air (it was a hot humid summer) condensed on the ducts downstream of the rotor and froze. Running the wind tunnel with dried air eliminated any condensation in the flow. Two disturbing effects due to the low temperature were observed. First, icing of the outer surface of the quartz glass windows was prohibited by blowing constantly dried pressurized air onto it. Secondly, thermal stresses in the test section occurred due to the temperature gradient over the rotor. This resulted in axial movements of hub, casing, stator and rotor. Superposed axial movements of stator and rotor resulted from the axial flow forces on both rows of airfoils. The stator and rotor positions were monitored during the measurements with the 3D-L2F by detecting the tips of stator and rotor leading and trailing edges and additionally a point on the outer casing. Figure 6 shows the stator and rotor movement over a six hours wind tunnel running period. The stator trailing edge at time 0 was set to x=0. Without flow and with non-rotating rotor the 3D-L2F detected a midspan axial gap (between stator trailing and rotor leading edge) of about 14.1 mm at time 0. This was consistent with previous manual measurements through the dismounted window using gage blocks. During the start up of the wind tunnel the casing and the stator moved downstream and the rotor upstream. This resulted in an axial gap of 13.7 mm after about one hour, when the measurements were started. The continuos cooling of hub and casing caused slight further movements of casing, stator and rotor around a mean value. The spatial measurement accuracy of the 3D-L2F is about $\pm$ 0.2 mm. The final reference values for stator and rotor positions were taken to be the mean of the measurements after one hour and at the end of the day.

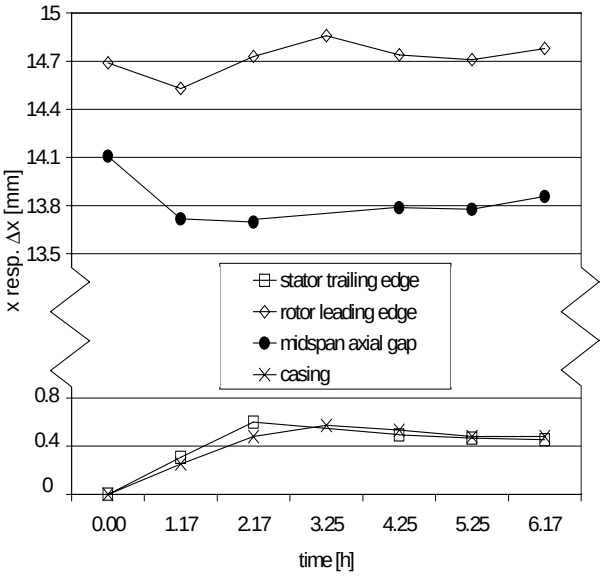

Fig. 6: *Movement of casing, stator and rotor*

ACCURACY ANALYSIS

Calculations of the measurement accuracy were performed based on a 95.5% confidence interval. Parts of the calculation are similar to those for steady flow conditions [Freudenreich and Fransson 1998]. The sources influencing the accuracy of the measurements can be subdivided into two parts:

System Inherent Accuracy Range

The sources for the system internal accuracy range are: Accuracy of the optical calibration, adjustment of the optical components and its alignment to the wind tunnel coordinate system, limited L2F electronic resolution. Compared to the first steady measurements [Freudenreich and Fransson 1998] some minor changes were done concerning the system inherent accuracy range:

- The accuracy of the radial flow angle χ depends on the measured difference $\alpha_{channel\ 2}$ - $\alpha_{channel\ 1}$. The accuracy of this measured difference transforms with a constant factor into the accuracy range of χ [Maass et al. 1994]. Based on a more recent publication by Vouillarmet and Charpenel [1998] this factor was increased from 4 to 5.
- Based on a series of very careful calibrations, the accuracy range of the calibration coefficients was approximated to zero.
- If the measurement volume has a finite extension in the circumferential direction Φ, flow gradients can occur over this extension. This can affect the radial flow angle χ. For the presented measurements this extension was minimized and any influence can be regarded to be eliminated. For a detailed description of this effect see Freudenreich and Fransson [1998].

Table 1 gives values for the system inherent accuracy ranges.

Statistical Accuracy Range

A statistical accuracy range results from a limited number of measured TOF events. The finally interesting values velocity, flow angle and turbulence intensity for both channels of the 3D-L2F are obtained from several TOF events being statistically evaluated. The higher the number of

evaluated TOF events per measurement position is the smaller the accuracy ranges are. Kost [1992b] suggested for the calculation of the accuracy range for normally distributed measurements

$$e_{statistical} = \frac{2 \cdot \sigma}{\sqrt{N}} \cdot \sqrt{1 + c \cdot \frac{\sigma_B^2}{A}} \qquad (2)$$

with σ as the standard deviation. According to Schodl [1986] it can be set equal to the measured turbulent flow quantities. N is the number of successfully evaluated TOF events. The first part of the equation, $2 \cdot \sigma / \sqrt{N}$, is the commonly known 95.5% confidence interval for normal distributions. The root part takes a superposed background noise level into account, where c is a weighting factor. The term σ_B^2 / A is the ratio of the squared variance of the background noise amplitude to the normal probability density distribution amplitude. This ratio could not be calculated directly based on the available information. Instead, it was considered as an inverse signal-to-noise ratio (SNR). During the statistical evaluation a flat noise band is stripped off from the finally used N TOF events. σ_B^2 / A was approximated by the ratio of totally obtained TOF events to the finally used N TOF events:

$$\frac{\sigma_B^2}{A} \sim \frac{\text{TOFs with noise}}{\text{TOFs without noise (N)}} \sim \frac{1}{SNR} + 1 \qquad (3)$$

The statistical accuracy range was calculated for all measured quantities at each local measurement position and for each time step. It resulted in smaller accuracy ranges than those ones for the stator measurements [Freudenreich and Fransson 1998] that were rather conservative estimations.

Total Accuracy Range

The 3D-L2F measures directly $\left|\vec{V}_{2D}\right|$. $\left|\vec{V}_{3D}\right|$ is calculated according to eq. (1). The influence of the accuracy ranges for $\left|\vec{V}_{2D}\right|$ and χ on the range of $\left|\vec{V}_{3D}\right|$ was calculated using the law of error propagation.

The separated accuracy ranges due to system inherent sources and the statistical evaluation are listed in Table 1. All accuracy ranges were regarded to be independent from each other. With the law of error propagation the total accuracy ranges were calculated to

$$e_{total} = \sqrt{\sum_{k=1}^{m} \left(e_k^2\right)} \qquad (4)$$

The statistical accuracy ranges depend strongly on the measurement position. Table 1 includes some representative examples of the statistical and total accuracy ranges of the unsteady measured quantities. The examples include stator wake and core flow in the axial gap, as well as rotor wake and core flow about one axial chord downstream of the rotor. For the rotor downstream position maximum occurring accuracy ranges were taken. Percentage values for the velocities are based on the local measured value in the absolute frame of reference. Percentage values for the turbulence intensity are absolute, as for the values for the two flow angles.

	$\left\|\vec{V}_{2D}\right\|$	$\left\|\vec{V}_{3D}\right\|$	α	χ	Tu
$e_{system\ inherent}$	±0.3%	±0.3%	±0.3°	±1.5°	+1%
$e_{statistical}$					
gap – core	±0.3%	±0.3%	±0.1°	±0.2°	±0.5%
gap – wake	±0.7%	±0.7%	±0.4°	±3.0°	±0.7%
rotor – core	±1.0%	±1.0%	±0.5°	±2.6°	±0.5%
rotor–wake	±2.0%	±2.0%	±2.0°	±9.9°	±1.7%
e_{total}					
gap – core	±0.4%	±0.4%	±0.3°	±1.5°	+ (0.8 - 1.2)%
gap – wake	±0.8%	±0.8%	±0.5°	±3.4°	+ (0.7 - 1.3)%
rotor – core	±1.0%	±1.0%	±0.6°	±3.0°	+ (0.8 - 1.2)%
rotor–wake	±2.0%	±2.0%	±2.0°	±10.0°	+ (0.0 - 2.0)%

Table 1: *Examples of accuracy ranges for unsteady measured quantities*

The accuracy ranges for $\left|\vec{V}_{2D}\right|$ and $\left|\vec{V}_{3D}\right|$ are identical (within the rounding accuracy) for all presented cases. Although the radial flow angle χ shows a relatively large accuracy range of more than 10°, no detectable influence is given on $\left|\vec{V}_{3D}\right|$.

RESULTS

Figures 7 and 8 show some examples of unsteady data including the accuracy ranges for each measurement point. Figure 7 shows $\left|\vec{V}_{3D}\right|$ in the rotor relative frame of reference at midspan about 1.5 mm upstream of the rotor leading edge. The graph covers exactly one rotor pitch. Rotor leading edges are located at $\Phi/\Phi_{Rotor} = 0$ and 1. The three graphs show the time-averaged flow and two instantaneous flow distributions, at 25% and 75% of a stator vane passing period. Both instantaneous graphs have slight kinks at $\Phi/\Phi_{Rotor} = 0.25$ for $t/T = 0.25$ and at $\Phi/\Phi_{Rotor} = 0.65$ for $t/T = 0.75$. These regions are affected by the stator wake. There, the accuracy range is increased compared to the other positions and to the time-averaged

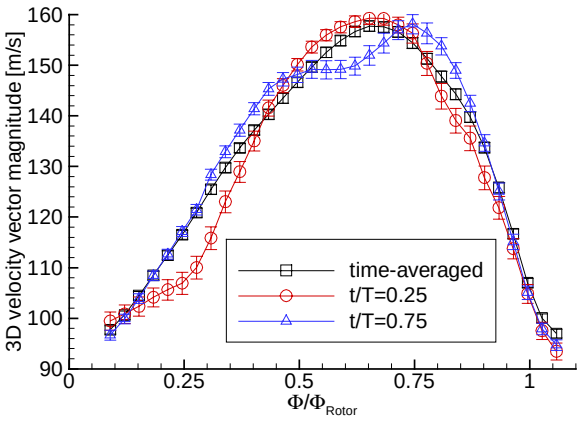

Fig. 7: *Time-averaged and instantaneous* $\left|\vec{V}_{3D}\right|$ *upstream of rotor*

flow. Figure 8 shows the radial flow angle χ one axial chord downstream of the rotor. The same three graphs are displayed as in Fig. 7. Between Φ/Φ_{Rotor} = 0.25 and 0.75 the flow is influenced by the rotor wake, resulting in stronger fluctuating radial flow angles and larger accuracy ranges.

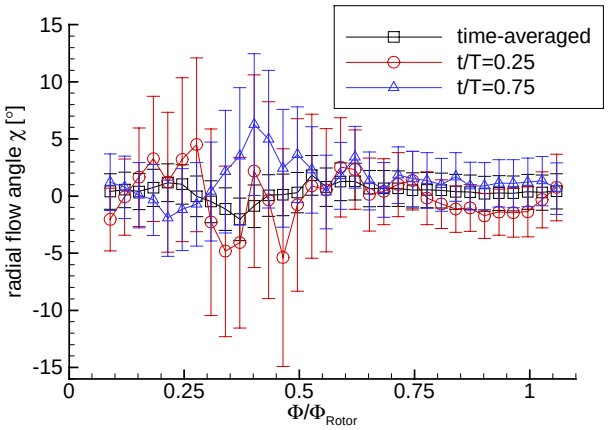

Fig. 8: *Time-averaged and instantaneous radial flow angle* χ *downstream of rotor*

ACKNOWLEDGEMENT

This work was initiated and supported by the European Community, Brite-Euram project "Aeromechanical Design of Turbine Blades" (ADTurB), contract number BEPR-CT95-0124.
The 3D-L2F system used in this investigation was acquired with funds provided by "Johnsonstiftelsen" and "Knut och Alice Wallenbergs Stiftelse", both in Sweden.
The authors wish to thank for the support by the Industrial Aerodynamics Section at DLR, especially Mr. Schüpferling, Mr. Tanger and Mr. Tappe for running the test facility and Dr. Kost for many fruitful discussions.

REFERENCES

Amecke, J.; Kost, F.; 1993
"Rotating Annular Cascades."
AGARD AG-328: "Advanced Methods for Cascade Testing.", 1993

Beversdorff, M.; Matziol, L.; Blaha, C.; 1998
"Application of 3D-Laser-Two Focus Velocimetry in Turbomachine Investigations."
AGARD CP-598: "Advanced Non-Intrusive Instrumentation for Propulsion Engines.", 1998

Binder, A; Förster, W.; Kruse, H.; Rogge, H.; 1985
"An Experimental Investigation into the Effect of Wakes on the Unsteady Turbine Rotor Flow."
Journal of Engineering for Gas Turbines and Power, Vol. 107, pp. 458-466, 1985 and ASME Paper No. 84-GT-178

Förster, W.; Schodl, R.; Kruse, H.; 1986
"Evaluation of L2F-Measurements in Unsteady Turbine Flow."
AGARD CP-399: "Advanced Instrumentation for Aero Engine Components." , 1986

Förster, W.; Schodl, R.; Beversdorff, M.; Klemmer, A.; Rijmenants, E.; 1990
"Design and Experimental Verification of 3D-Velocimeters based on the Laser-2-Focus Technique."
5th Int. Symp. on Appl. of Laser Anemometry to Fluid Mechanics, Lisbon, Portugal, 1990

Freudenreich, K.; Fransson, T. H.; 1998
"Application of Three Dimensional Laser-Two-Focus Anemometry to Transonic Turbine Flows: Example of an Isolated Stator."
14th Symposium on Measuring Techniques for Transonic and Supersonic Flow in Cascades and Turbomachines, Limerick, Ireland, 1998

Freudenreich, K.; Jöcker, M.; Rheder, H.-J.; Höhn, W.; Fransson, T.H.; 1999
"Aerodynamic Performance of Two Isolated Stators in Transonic Annular Cascade Flow."
Paper No. 557/063/99, 3rd European Conference on Turbomachinery, London, UK, 1999

Gieß, P.-A.; Kost, F.; 1997
"Detailed Experimental Survey of the Transonic Flow Field in a Rotating Annular Turbine Cascade."
2nd European Conference on Turbomachinery, Antwerp, Belgium, 1997

Kost, F., 1992a
"Three Dimensional Transonic Flow Measurements in an Axial Turbine with Conical Walls."
ASME Paper No. 92-GT-61, 1992

Kost, F.; 1992b:
"A Study of some Measurement Errors in L2F-Velocimetry."
11th Symposium on Measuring Techniques for Transonic and Supersonic Flow in Cascades and Turbomachines, Munich, Germany, 1992

Kost, F.; 1996
"Improvements in the Application of Laser-Two-Focus Velocimetry to Transonic Rotor Flows."
13th Symposium on Measuring Techniques for Transonic and Supersonic Flow in Cascades and Turbomachines, Zürich, Switzerland, 1996

Kost, F.; Hummel, F.; Tiedemann, M.; 2000
"Investigation of the Unsteady Rotor Flow Field in a Single HP Turbine Stage."
ASME Paper No. 2000-GT-0432, 2000

Maass, M.; Förster, W.; Thiele, P.; 1994
"Unsteady Flow Experiments in the Exit of a Ducted Propfan Rotor."
AIAA Paper No. 94-2970, 1994

Schodl, R.; 1980
"A Laser-Two-Focus (L2F) Velocimeter for Automatic Flow Vector Measurements in the Rotating Components of Turbomachines."
Journal of Fluids Engineering, Vol. 102 pp. 412-419, 1980

Schodl, R.; 1986
"Laser-Two-Focus Velocimetry."
AGARD CP-399: "Advanced Instrumentation for Aero Engine Components." , 1986

Trebinjac, I.; Vouillarmet, A.; Perrin, G.; 1993
"A Contribution to the Understanding of the Flow Field in a Supersonic Compressor."
2nd International Symposium on Experimental and Computational Aerothermodynamics of Internal Flows, Prague, Czech Republic, 1993

Vouillarmet, A.; Charpenel, S.; 1998
"Laser Two Focus Anemometry (L2F-3D) for Three-Dimensional Flow Analysis in an Axial Compressor."
AGARD CP-598: "Advanced Non-Intrusive Instrumentation for Propulsion Engines.", 1998

Walraevens, R. E.; Gallus, H. E.; 1995
"Stator-Rotor-Stator Interaction in an Axial Flow Turbine and ist Influence on Loss Mechanisms."
AGARD CP-571: "Loss Mechanisms and Unsteady Flow in Turbomachines.", 1995

Zaccaria, M. A.; Lakshminarayana, B.; 1997
"Unsteady Flow Field due to Nozzle Wake Interaction with the Rotor in an Axial Flow Turbine: Part I - Rotor Passage Flow Field."
Journal of Turbomachinery Vol. 119, pp. 201-213, 1997 and ASME Paper No. 95-GT-295